

# Synthesis and luminescence properties of nanocrystalline $\text{YVO}_4:\text{Eu}^{3+}$

Li Yanhong<sup>a,b</sup>, Hong Guangyan<sup>a,\*</sup>

<sup>a</sup>Key Laboratory of Rare Earth Chemistry and Physics, Changchun Institute of Applied Chemistry, Graduate School of the Chinese Academy of Sciences, Chinese Academy of Sciences, No. 5625, Renmin Street, Changchun City, Jilin Province 130022, China

<sup>b</sup>College of Materials and Chemical Engineering, Changchun University of Science and Technology, Changchun 130022, China

Received 27 October 2004; received in revised form 1 December 2004; accepted 7 December 2004

## Abstract

Nanocrystalline  $\text{YVO}_4:\text{Eu}^{3+}$  was synthesized by direct precipitation reaction, which was then annealed at different temperatures. The results of XRD showed that nanocrystalline  $\text{YVO}_4:\text{Eu}^{3+}$  could be obtained in solution at 60 °C, and the mean particle sizes of samples are increased as annealing temperature is increased. The results of TEM exhibit that the sizes of samples are around 5–30 nm. Studies on the excitation spectra show that there are a large number of the structural distortions in smaller particles. By analyzing line splitting patterns and peaks broadening in the emission spectra, we consider that the deviations in intensity patterns of  $^5\text{D}_0\text{--}^7\text{F}_2$  are affected by distortions of crystal lattice. Some abnormal behaviors can be attributed to higher ratio of surface to volume, which lead to the different local symmetry environment of  $\text{Eu}^{3+}$  ions on the surface.

© 2005 Elsevier Inc. All rights reserved.

**Keywords:** Nanocrystalline  $\text{YVO}_4:\text{Eu}^{3+}$ ; Direct precipitation reaction; Excitation spectra; Emission spectra

## 1. Introduction

In recent years, rare-earth-doped nanocrystalline phosphors have attracted great interest. The main work concerns the synthesis and the spectrum changes of nanoparticles. The results of much work indicate that the surface and the lattice distortions play important roles in luminescent properties of nanocrystals. It is well known that the differences of local structure of  $\text{Eu}^{3+}$  ions should lead to spectral changes for decreased grain size. The luminescence spectrum of  $\text{Eu}^{3+}$  ions itself can be used to probe its crystal environment, about which a large number of studies have been achieved [1–8]. Among the different host materials researched, much attention has been given to  $\text{YVO}_4:\text{Eu}^{3+}$ , which was used as red phosphor in color television cathode ray tube displays and high pressure mercury lamps, not only because bulk materials exhibit a high luminescence

efficiency, but also because it can be crystallized at low temperatures to obtain much smaller nanocrystals easily [9–16].

Different methods have been used to prepare  $\text{YVO}_4:\text{Eu}^{3+}$  since it was introduced by Levine and Pallia in 1964 [17], for example, high temperature solid state method [18], hydrolyzed colloid reaction technique [19], solution combination method [20], hydrothermal methods [8,10] and urea precipitation technique [21], etc. Among these techniques, wet chemistry methods have been shown to be very powerful technique to prepare well-dispersed nanoparticles with a controlled size, shape, and surface state. However, either synthesis routes are complicated, or spectrum investigations are based on the colloidal aqueous solutions, in which  $\text{OH}^-$  ions quench the emission from  $\text{Eu}^{3+}$  ions.

In this paper, a simple direct precipitation method was adopted to synthesize  $\text{YVO}_4:\text{Eu}^{3+}$  nanoparticles by considering the reaction mechanism of vanadate, and the structures and the luminescence spectra of  $\text{YVO}_4:\text{Eu}^{3+}$  nanoparticles were investigated.

\*Corresponding author. Fax: +86 431 5698 041.

E-mail address: [gyhong@ciac.jl.cn](mailto:gyhong@ciac.jl.cn) (H. Guangyan).

## 2. Experimental section

$\text{YVO}_4:\text{Eu}^{3+}$  nanoparticles were prepared by direct precipitation reaction, because the formation of vanadate groups is sensitive to the pH of solution, and the dependence of particle size on pH has been investigated earlier [10–12]. Optimization of the experimental conditions led us to choose the following experimental conditions:

A solution of  $\text{NH}_4\text{VO}_3$  (40 ml; 0.05 mol/L) was adjusted to pH 12.5 with NaOH. The mixture of solution of  $\text{Y}(\text{NO}_3)_3$  (38 ml; 0.05 mol/L) and  $\text{Eu}(\text{NO}_3)_3$  (2 mL; 0.05 mol/L) were added dropwise, a yellow opalescent colloid was observed, and the pH of solution was stabilized at about 8 after 10 min. The colloids were subsequently heated to 60 °C for 1 h with magnetic stirring, a milky colloid containing the nanocrystalline  $\text{YVO}_4:\text{Eu}^{3+}$  has been obtained. Nanoparticles were separated from the reaction solution by filtering, and washed with distilled water for several times; finally, powders of the nanocrystalline  $\text{YVO}_4:\text{Eu}^{3+}$  were obtained by drying at 60 °C in an air atmosphere. In order to investigate the structure and luminescence properties of nanoparticles, different portions of powders were heated at 300, 400 and 600 °C for 2 h, respectively.

The structures of the products were recorded with an RIGAKU D/MAX II B X-ray powder diffractometer with  $\text{CuK}\alpha$  ( $\lambda = 0.15406 \text{ nm}$ ) radiation generated at 40 kV/20 mA. The morphology of obtained samples was studied with a JEOL JEM-2010 transmission electron microscope operated at 200 kV. Photoluminescence was observed with a Hitachi F-4500 fluorescence spectrophotometer equipped with a 150 W Xe lamp at room temperature.

## 3. Results and discussion

### 3.1. Structural characterization of the nanoparticles

The XRD pattern of nanocrystalline  $\text{YVO}_4:\text{Eu}^{3+}$ , as well as ones annealed at different temperatures, is shown in Fig. 1, which can be indexed as tetragonal zircon structure (JCPDS File No.17-0341). The results exhibit that pure phase  $\text{YVO}_4:\text{Eu}^{3+}$  can be obtained at 60 °C, and the diffraction intensities of samples are increased due to much better crystallization as annealing temperature is increased. By applying the Scherrer formula to the full width at half maximum of the (200) diffraction peak, the mean particle sizes could be calculated as 5, 10, 12 and 18 nm for initial nanoparticles and the samples annealed at 300, 400 and 600 °C, respectively. Obviously, the grain sizes of  $\text{YVO}_4:\text{Eu}^{3+}$  samples depend on the annealing temperature.

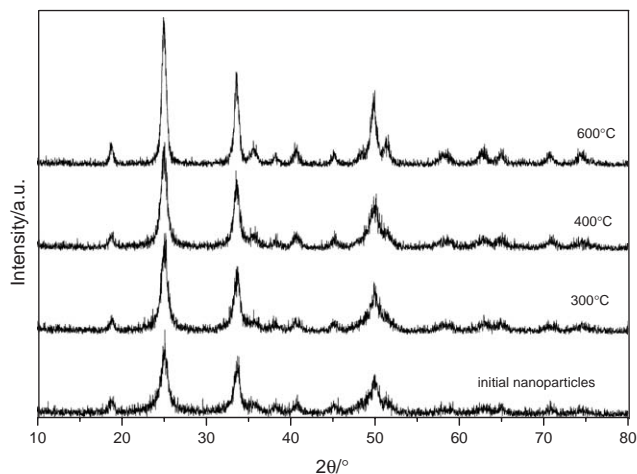


Fig. 1. XRD patterns of  $\text{YVO}_4:\text{Eu}^{3+}$  nanoparticles.

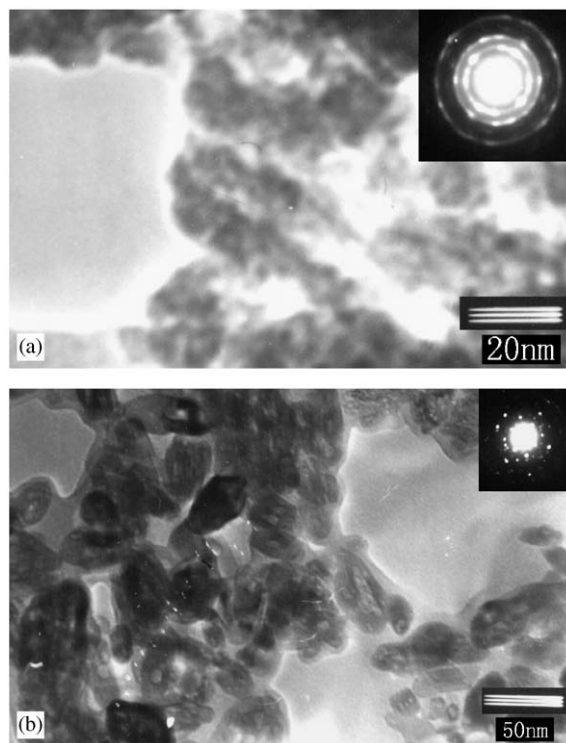


Fig. 2. The TEM images of samples prepared at different temperatures: (a) at 60 °C, (b) annealed 600 °C.

Fig. 2 shows the TEM images of samples prepared at different temperatures (60, 600 °C), the mean particle sizes estimated were 5 and 25 nm, respectively, the primary crystal sizes are consistent with the results from XRD, however, there is a tendency to agglomerate larger particles for the initial nanoparticles (Fig. 2a). Ellipsoidal particles annealed at 600 °C consist of numerous small particles, this is a consequence of the aggregation of primary particles. The results also display

that more defects may exist in the annealed nanoparticles. The electron diffraction patterns are shown in the inset of Fig. 2a and b, further confirming the structure of the nanoparticles, indicating much better crystallization occurred as annealing temperature increased.

### 3.2. Optical properties of the nanoparticles

The excitation spectra of the nanoparticles  $\text{YVO}_4:\text{Eu}^{3+}$  monitored at 614 nm, are shown in Fig. 3a. Excitation spectra of four examples exhibit a strong broad overlap absorption in the range of 200–360 nm, which are assigned to charge transfer bands of Eu–O and V–O. Much weaker narrow bands in the range of 360–500 nm correspond to direct excitation of the  $\text{Eu}^{3+}$  ions of 4f manifold ( ${}^7\text{F}_{0,1}-{}^5\text{D}_4$ ,  ${}^7\text{F}_{0,1}-{}^5\text{G}_j$ ,  ${}^5\text{L}_7$ ,  ${}^7\text{F}_{0,1}-{}^5\text{L}_6$ ), consistent with spectral characterizations observed in previous work [1,8]. Some small differences can be observed. First, for the charge transfer band, except when the excitation

intensity increase with the increasing treatment temperature, it is clear that the charge transfer band of V–O systematically shifts to longer wavelength with increasing annealing temperature. The reason for these alterations may be due to lattice distortions, because the V–O average distances for smaller nanoparticles are longer than for larger nanoparticles, and the excitation energy required is higher for  $\text{V}^{+5}\text{O}_n^{-2n} \rightarrow \text{V}^{+4}\text{O}_n^{-2n+1}$ ; Second, for the direct excitation band of  $\text{Eu}^{3+}$  ions, it is very interesting that the intensity and width order of excitation peaks for different samples have different; the enlarging excitation spectra from 360 to 500 nm are shown in Fig. 3b. This results from two competitive effects: the amount of  $\text{Eu}^{3+}$  ions with disorder on the surface and much better crystallization. Considering higher surface/volume ratios in nanocrystals, more  $\text{Eu}^{3+}$  ions locate on the surface or near the surface with disorder compared to interior  $\text{Eu}^{3+}$  ions. These reasons lead to the higher intensity and the broader excitation band for initial nanoparticles. When the annealing temperature is increased, nanoparticles grow, which reduces the  $\text{Eu}^{3+}$  ions on the surface. This makes the excitation intensity weaker for samples annealed at 300 and 400 °C, however, the excitation intensity of samples annealed at 600 °C become stronger. This is because more  $\text{Eu}^{3+}$  ions on the surface have occupied the order lattice site due to obtain energy enough.

In  $\text{YVO}_4$  structure, the  $\text{Eu}^{3+}$  ions have  $\text{D}_{2d}$  symmetry with the absence of an inversion center. The splitting patterns of energy levels have been calculated. As reported in previous work, for the bulk  $\text{YVO}_4:\text{Eu}^{3+}$ , the emission spectra mainly consists of  ${}^5\text{D}_0-{}^7\text{F}_2$  (a typical electric dipole transition) and  ${}^5\text{D}_0-{}^7\text{F}_1$  (a typical magnetic dipole transition), and the emission of vanadate groups have been quenched due to effective transfer energy to  $\text{Eu}^{3+}$  ions instead of  $\text{Y}^{3+}$  ions [8–9,15].

Fig. 4 displays the emission spectra of the nanoparticles prepared at different temperatures. It is noticed that the splitting patterns of  ${}^5\text{D}_0-{}^7\text{F}_j$  transitions in nanoparticles are corresponding to the bulk materials, no obvious vanadate groups emission band can be seen, this indicates that excited vanadate groups have completely transferred energy to  $\text{Eu}^{3+}$  by phonons. We can confirm that europium ions occupy the host lattice instead of  $\text{Y}^{3+}$  ions, although nanoparticles were synthesized at 60 °C. By comparison, the relatively intensity patterns of the lines belonging to the  ${}^5\text{D}_0-{}^7\text{F}_2$  transition,  ${}^5\text{D}_0-{}^7\text{F}_2$  (doubly degenerated E state) and  ${}^5\text{D}_0-{}^7\text{F}_2$  (the singlet  $\text{B}_2$  state), respectively, are different from that in the bulk. It is well known that the oscillator strength of these transitions is affected by distortions that obey selection rules for electromagnetic transitions in dodecahedral symmetry [15]. Thereby, the distortions in nanocrystalline  $\text{YVO}_4:\text{Eu}^{3+}$  synthesized in the solution at 60 °C may exist, and influence the luminescence spectra.

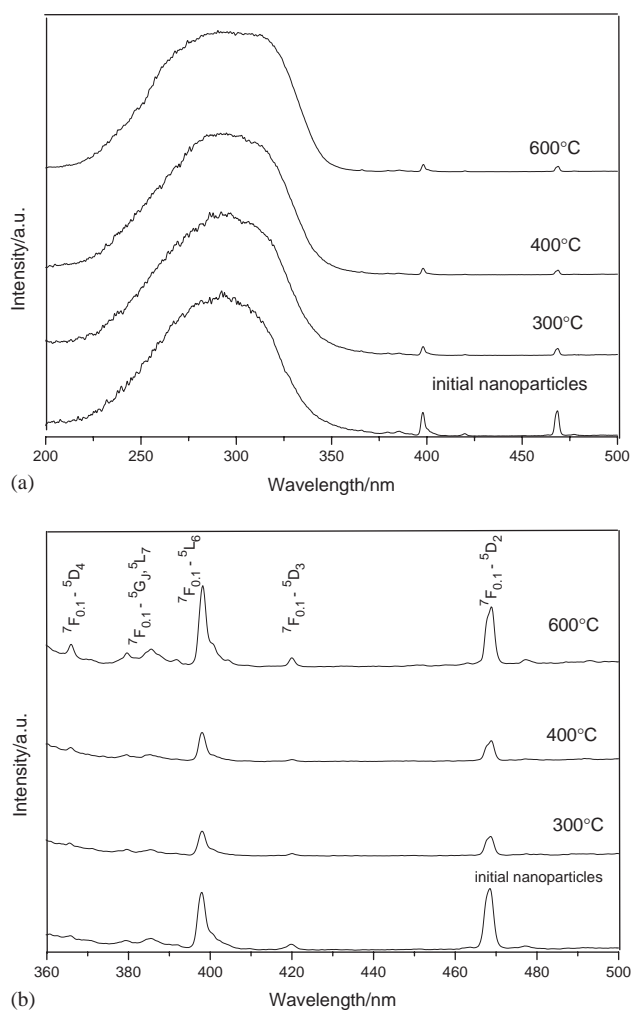


Fig. 3. The excitation spectra of the nanoparticles  $\text{YVO}_4:\text{Eu}^{3+}$ : (a) Excitation spectra from 200 to 500 nm. (b) Excitation spectra from 360 to 500 nm.

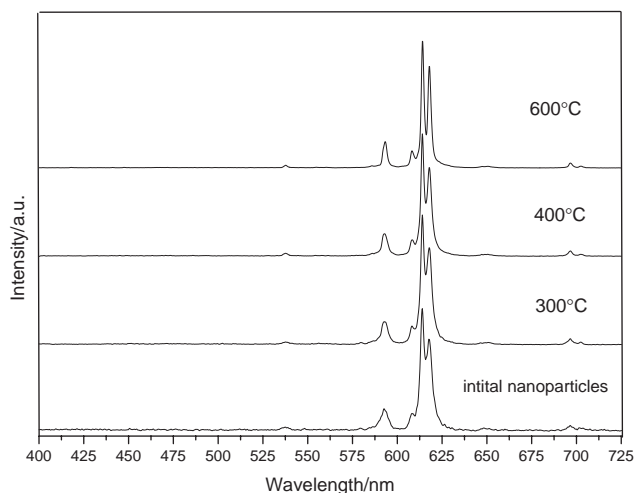


Fig. 4. Emissions spectra of  $\text{YVO}_4:\text{Eu}^{3+}$  nanoparticles (Under 293 nm excitation).

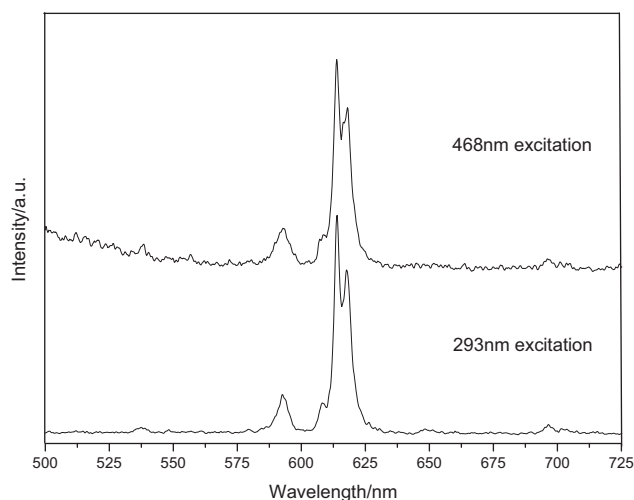


Fig. 5. Emissions spectra of  $\text{YVO}_4:\text{Eu}^{3+}$  initial nanoparticles (Under 293 and 468 nm excitation).

Similarly the  ${}^5\text{D}_0\text{-}{}^7\text{F}_1/{}^5\text{D}_0\text{-}{}^7\text{F}_2$  intensity ratios show that the environment of  $\text{Eu}^{3+}$  ion is almost the same in all nanoparticles synthesized. The slightly broaden emission peaks for initial nanoparticles are observed, and the tendency of a broadened emission peak is reduced with temperature increase, this is possibly related to some structure distorts due to lower crystalline temperature.

Fig. 5 displays emission spectra of initial nanoparticles, which were excited by the 293 and 468 nm, respectively. It is observed that broad emission bands with stronger relative intensity of  ${}^5\text{D}_0\text{-}{}^7\text{F}_1$  transition are revealed under 468 nm excitation, whereas these features are much weaker under 293 nm excitation. All these results are associated with the different local symmetry

environment of  $\text{Eu}^{3+}$  ions excited. These behaviors can be attributed to a higher ratio of surface to volume and a larger number of defects on the surface.

#### 4. Conclusions

$\text{YVO}_4:\text{Eu}^{3+}$  nanoparticles were prepared by direct precipitation reactions, and annealed at 300, 400 and 600 °C. The results of XRD show that nanocrystalline  $\text{YVO}_4:\text{Eu}^{3+}$  can be obtained in solution at 60 °C, and the grain sizes of  $\text{YVO}_4:\text{Eu}^{3+}$  depend on the annealing temperature. The morphology was determined with TEM, which found that the sizes of samples were around 5–30 nm. The excitations and emission spectra were studied. Some differences in spectra for the smaller nanoparticles synthesized can be seen, such as alteration of charge transfer band, abnormal intensity order of direct excitation lines of the  $\text{Eu}^{3+}$  ions in excitation spectra for different samples, broadening peaks in the emission spectra, and different relative intensity belong to  ${}^5\text{D}_0\text{-}{}^7\text{F}_2$  in emission spectra. We can conclude that structural distortions and defects existed in the small particles of samples synthesized, and the characteristics of  $\text{Eu}^{3+}$  ions relate to different local symmetry environment.

#### References

- [1] H. Meysamy, K. Riwotzki, A. Kornowski, S. Nased, M. Haase, Wet chemical synthesis of doped colloidal nanomaterials: particles and fibers of  $\text{LaPO}_4:\text{Eu}$ ,  $\text{LaPO}_4:\text{Ce}$ , and  $\text{LaPO}_4:\text{Ce, Tb}$ , *Adv. Mater.* 11 (1999) 840–844.
- [2] M. Haasw, K. Riwotzki, H. Meysamy, A. Kornowski, Synthesis and properties of colloidal lanthanide-doped nanocrystals, *J. Alloys Compd.* 303–304 (2000) 191–197.
- [3] R.Y. Wang, Distribution of  $\text{Eu}^{3+}$  ions in  $\text{LaPO}_4$  nanocrystals, *J. Lumin.* 106 (2004) 211–217.
- [4] Z. Wei, L. Sun, C. Liao, C. Yan, Fluorescence intensity and color purity improvement in nanosized  $\text{YBO}_3:\text{Eu}$ , *Appl. Phys. Lett.* 80 (2002) 1447–1449.
- [5] L.D. Sun, J. Yao, C.H. Liu, et al., Rare earth activated nanosized oxide phosphors: synthesis and optical properties, *J. Lumin.* 87–89 (2000) 447–450.
- [6] J. Dhanaraj, R. Jagannathan, T.R.N. Kutty, et al., Photoluminescence characteristics of  $\text{Y}_2\text{O}_3:\text{Eu}^{3+}$  nanophosphors prepared using sol-gel thermoses, *J. Phys. Chem. B.* 105 (2001) 11098–11105.
- [7] H. Peng, H. Song, B. Chen, S. Lu, S. Huang, Spectral difference between nanocrystalline and bulk  $\text{Y}_2\text{O}_3:\text{Eu}^{3+}$ , *Chem. Phys. Lett.* 370 (2003) 485–489.
- [8] K. Riwotzki, M. Haase, Wet chemical synthesis of doped colloidal nanoparticles:  $\text{YPO}_4:\text{Lu}$ , ( $\text{Ln} = \text{Eu, Sm, Dy}$ ), *J. Phys. Chem. B* 102 (1998) 10129–10135.
- [9] C.H. Yan, L.D. Sun, C.S. Liao,  $\text{Eu}^{3+}$  ion as fluorescent probe for detecting the surface effect in nanocrystals, *Appl. Phys. Lett.* 82 (2003) 3511–3513.
- [10] H. Wu, H. Xu, Q. Su, T. Chen, M. Wu, Size and shape tailored hydrothermal synthesis of  $\text{YVO}_4$  crystals in ultra wide pH range conditions, *J. Mater. Chem.* 13 (2003) 1223–1228.

- [11] A. Huignard, V. Burssette, G. Laurent, T. Gacoin, J.P. Boilot, Synthesis and characterizations of  $\text{YVO}_4$ : Eu colloids, *Chem. Mater.* 14 (2002) 2264–2269.
- [12] L. Dong Sun, Y. Xin Zhang, J. Zang, C. Yan, C. Liao, Y. Lu, Fabrication of size controllable  $\text{YVO}_4$  nanoparticles via micro-emulsion-mediate synthetic process, *Solid State Commun.* 124 (2002) 35–38.
- [13] A. Huignard, T. Gacoin, J.-P. Boilot, Synthesis and luminescence properties of colloidal  $\text{YVO}_4$ : Eu phosphors, *Chem. Mater.* 12 (2000) 1090–1094.
- [14] M. Yu, J. Lin, Z. Wang, J. Fu, S. Wang, H.J. Zhang, Y.C. Han Fabrication, Patterning, and optical properties of nanocrystalline  $\text{YVO}_4$ : a phosphor films via sol-gel soft lithography, *Chem. Mater.* 14 (2000) 2224–2231.
- [15] A. Huignard, V. Burssette, A.-C. Francille, T. Gacoin, J.-P. Boilot, Emission processed in  $\text{YVO}_4$ : eunanoparticels, *J. Phys. Chem. B.* 107 (2003) 6754–6759.
- [16] H.Y. Xu, H. Wang, Y.Q. Meng, H. Yan, Rapid synthesis of size-controllable  $\text{YVO}_4$  nanoparticles by microwave irradiation, *Solid State Commun.* 130 (2004) 465–468.
- [17] A.K. Levine, F.C. Palilla, *Appl. Phys. Lett.* 5 (1964) 118.
- [18] R.C. Ropp, Spectra of some rare earth vanadates, *J. Electrochem. Soc.: Solid State Sci.* 115 (1968) 940–945.
- [19] S. Erdei, Preparation of  $\text{YVO}_4$  powder from the  $\text{Y}_2\text{O}_3 + \text{V}_2\text{O}_5 + \text{H}_2\text{O}$  system by a hydrolyzed colloid reaction (HCR) technique, *J. Mater. Sci.* 30 (1995) 4950–4959.
- [20] F.M. Nirwan, T.K. Gundu Rao, P.K. Gupta, R.B. Pode, Studies of defects in  $\text{YVO}_4\text{Pb}^{2+}$ ,  $\text{Eu}^{3+}$  red phosphor materials, *Phys. Stat. Sol. (a)* 198 (2003) 447–456.
- [21] A. Newport, J. Silver, A. Vecht, The synthesis of fine particle yttrium vanadate phosphors from spherical powder precursors using urea precipitation, *J. Electrochem. Soc.* 147 (2000) 3944–3947.